Stable and Selective Electrochemical Reduction of Carbon Dioxide to Ethylene on Copper Mesocrystals

Journal:	*Catalysis Science & Technology*
Manuscript ID:	CY-ART-07-2014-000906.R1
Article Type:	Paper
Date Submitted by the Author:	08-Aug-2014

Complete List of Authors:	Chen, Chung Shou; National University of Singapore, Chemistry Handoko, Albertus; National University of Singapore, Chemistry Wan, Jane Hui; National University of Singapore, Chemistry Ma, Liang; National University of Singapore, Chemistry Ren, Dan; National University of Singapore, Chemistry Yeo, Boon Siang; National University of Singapore, Department of Chemistry

Cite this: DOI: 10.1039/c0xx00000x

www.rsc.org/xxxxxx

ARTICLE TYPE

Stable and Selective Electrochemical Reduction of Carbon Dioxide to Ethylene on Copper Mesocrystals†

Chung Shou Chen,[a] Albertus D. Handoko,[a] Jane Hui Wan,[a] Liang Ma,[a] Dan Ren[a] and Boon Siang Yeo*[,a]

Received (in XXX, XXX) Xth XXXXXXXXX 20XX, Accepted Xth XXXXXXXXX 20XX

DOI: 10.1039/b000000x

Stable and selective electrochemical reduction of carbon dioxide to ethylene was achieved using copper mesocrystal catalysts in 0.1 M $KHCO_3$. The Cu mesocrystal catalysts were facilely derived by the *in-situ* reduction of a thin CuCl film during the first 200 seconds of the CO_2 electroreduction process. At -0.99 V vs. RHE, the Faradaic efficiency of ethylene formation using these Cu mesocrystals was ~18× larger than that of methane, and forms up to 81% of the total carbonaceous products. Control CO_2 reduction experiments show that such selectivity towards C_2H_4 formation could not be replicated by using regular copper nanoparticles formed by pulsed electrodeposition. High resolution transmission electron microscopy reveals the presence of both $(100)_{Cu}$ facets and atomic steps in the Cu mesocrystals, which we assign as active sites in catalyzing the reduction of CO_2 to C_2H_4. CO adsorption measurements suggest that the remarkable C_2H_4 selectivity could be attributed to the greater propensity of CO adsorption on Cu mesocrystals, as compared to on other types of Cu surfaces. The Cu mesocrystals remained active *and* selective towards C_2H_4 formation for longer than *six hours*. This is an important and industrially relevant feature missing from many reported Cu-based CO_2 reduction catalysts.

Introduction

Carbon dioxide reduction to hydrocarbons and alcohols has the potential of generating a sustainable supply of valuable feedstock for our chemical industries and fuels for our energy needs.[1] This process also mitigates excessive CO_2 buildup in the atmosphere which contributes to global climate warming. CO_2 can be electrochemically reduced to hydrocarbons such as ethylene and methane via $2CO_2 + 12e^- + 8H_2O \rightarrow C_2H_4 + 12OH^-$ and $CO_2 + 8e^- + 6H_2O \rightarrow CH_4 + 8OH^-$ respectively. C_2H_4 is a particularly valuable product as it has widespread applications in many industries including agriculture and polymer manufacturing. To date, the most promising catalyst that can electroreduce CO_2 to C_2H_4 is copper metal.[2, 3] However, alongside C_2H_4, many carbonaceous side-products including methane (CH_4), carbon monoxide (CO) and formate ($HCOO^-$) are also simultaneously formed.[4-7] The Cu catalysts are furthermore highly susceptible to poisoning and deactivation, commonly within 30 minutes from the start of the CO_2 reduction process.[8, 9] For the above reasons, considerable effort has been dedicated to understanding the structure and composition of materials with the aim of developing catalysts that can selectively reduce CO_2 to C_2H_4 over a long period of time.[7, 10, 11]

Polycrystalline Cu surfaces do not show significant preference towards ethylene formation, with C_2H_4/CH_4 product ratio of around 1 to 2.[3-5, 12, 13] It is thought that the lack of selectivity originates from the great heterogeneity of sites present on the polycrystalline surface, each with different catalytic activities. This is underscored by the work of Hori et al., who investigated the effect of different Cu facets on the selectivity of CO_2 electroreduction.[7, 14] Single crystal $(100)_{Cu}$ surfaces were found to favor the formation of C_2H_4 more than $(111)_{Cu}$, as indicated by their C_2H_4/CH_4 ratios of 1.3 and 0.2 respectively.[7] Interestingly, when high-indexed $(711)_{Cu}$, $(911)_{Cu}$, and $(810)_{Cu}$ planes, formed by cleaving $(100)_{Cu}$, were examined, they displayed even higher selectivity towards C_2H_4 with the C_2H_4/CH_4 ratio value increasing to 10 for $(711)_{Cu}$. Whether the selectivity is due to increased population of atomic steps exposed in such high-indexed facets or a certain periodic spacing in the exposed copper terraces, it is clear that certain Cu facets do exhibit preference towards different hydrocarbons and it is possible to tune them.

Beside single crystal Cu surfaces, enhancements in C_2H_4 selectivity during CO_2 reduction were also observed on CuO and Cu^I-halide coated electrodes.[15, 16] Sustaining stable catalytic activities on these catalysts is however more challenging, because Cu^{II} or Cu^I will inevitably reduce to Cu metal during the CO_2 reduction process. Thus, in the case of Cu oxide, intermittent anodic pulses of +1 to +2 V had to be applied during the CO_2 reduction process to maintain the Cu oxide in its catalytic active oxidative state.[15] Large cathodic potentials of up to -3 V (vs. Ag/AgCl) were also required for the CO_2 reduction process, which significantly increased the energy input of the system. High surface area Cu nanoparticles have been shown to offer good selectivity towards hydrocarbon formation, especially C_2H_4.[6] It was proposed that the numerous steps and edges formed on the surfaces of the Cu nanoparticles could be crucial for selective C_2H_4 formation. In support of this, quantum chemical simulations indicated that reaction intermediates like CHO* are

more stable on the steps of $(211)_{Cu}$ surface than $(100)_{Cu}$ terrace. This could lead to their concentration build up and eventual dimerization to C_2H_4.[17] More recently, thick Cu_2O films have also shown promising selectivity towards C_2H_4 formation[18] Local pH changes associated with thickness of the films was proposed to induced such selectivity, as pH has been shown to alter production rates of various CO_2 reduction products.[10]

These preceding works have inspired us to develop stable C_2H_4-selective electrocatalyst based on copper and understand how such selectivity came to fruition. Herein, we report the activity and characteristics of novel copper mesocrystals for the selective electroreduction of CO_2 to C_2H_4. These mesocrystals were facilely prepared by electrochemically roughening a Cu electrode in KCl electrolyte to give a thin overlayer of CuCl. The CuCl was then reduced in situ during the CO_2 electroreduction process to yield Cu mesocrystals. These catalysts are highly active for CO_2 reduction to C_2H_4, which was demonstrated by the high C_2H_4/CH_4 Faradaic efficiency (FE) ratio of ~18. The FE of C_2H_4 forms up to ~81% of the total carbonaceous products. Thorough materials analysis reveal that the morphology of these mesostructurally arranged 30-50 nm copper particles displayed both $(100)_{Cu}$ facets and numerous steps/edges. Cyclic voltammetry studies indicate that the C_2H_4 selectivity on these mesocrystals can be correlated to the propensity and stronger adsorption of CO intermediates on its surfaces. Control experiments performed on copper nanoparticles prepared by pulsed electro-deposition or electropolished Cu surfaces show that such selectivity could not be simply replicated by ordinary nanoparticulate or bulk copper surfaces.

Our results demonstrate that *both* $(100)_{Cu}$ facets and steps formed on copper mesocrystals are *essential* for the selective reduction of CO_2 to C_2H_4. These copper mesocrystals remain very active and selective for C_2H_4 production for over *six hours*. They are also robust enough to be taken out mid reaction, exposed to the environment and reintroduced to fresh electrolyte for a full round of CO_2 electroreduction without significant loss in activity. Addition of Cl^- in the electrolyte did not affect the activity of the copper mesocrystals significantly. Our discovery of a facilely prepared, robust and selective catalyst based on an earth-abundant metal such as Cu represents a major step forward for the realization of industrial-scale reduction of CO_2 to C_2H_4.

Experimental

Catalyst Preparation

Only deionized Type I water (18.2 MΩ cm, Barnstead, Thermo Scientific) was used for washing and for preparing solutions. 10 mm diameter Cu metal discs (99.99%, Goodfellow Inc.) were used as the base to prepare all catalysts. These discs were mechanically polished with SiC paper and alumina slurries, resulting in a mirror-like finish.[19] Between each step, the copper discs were ultrasonicated in deionized water and 0.1 M KOH to remove any alumina particles left on their surface.

The following catalysts were prepared:

1. Catalyst A: Cu mesocrystals. Polished copper discs were electrochemically roughened in aqueous 0.1 M KCl using five triangular potential scans ranging from 0.24 V to 1.74 V (vs. RHE) at a rate of 500 mV s^{-1}. During each cycle, the potential was held at the positive and negative limits for 10 and 5 seconds respectively. They were then rinsed and washed in copious amount of deionized water several times. Cu mesocrystals were then formed in-situ during the CO_2 electroreduction process in CO_2-saturated 0.1 M $KHCO_3$ (99.99%, Sigma Aldrich). These parameters were the optimum for obtaining a mechanically stable layer of Cu mesocrystals. This sample shall be addressed in this article as Catalyst A or Cu mesocrystals.

2. Catalyst B: Cu nanoparticles. Cu nanoparticles were electrodeposited on polished Cu discs using 3000 cycles of galvanostatic pulse deposition. Square wave pulsed current setting was used, alternated between −4.94 and +2.49 mA cm^{-2}, with 100 ms duration for both anodic and cathodic pulses. The electrolyte consisted of 0.01 M $CuSO_4$ (extra pure, GCE Laboratory Chemicals), 0.1 M Na_2SO_4 (≥99.0%, Sigma Aldrich) and 0.1 M H_2SO_4 (98%, RCI Labscan). This sample shall be addressed as Catalyst B or Cu nanoparticles.

3. Catalyst C: Electropolished Cu. Mechanically-polished Cu disks were electropolished in phosphoric acid (85%, RCI Labscan) at 259.7 mA cm^{-2} anodic current for 60 seconds and then rinsed with deionized water.[6] This sample shall be addressed as Catalyst C or electropolished Cu.

Online Electrochemical Gas Chromatography (GC)

Electrochemical measurements were performed using a Gamry 600 galvanostat/potentiostat in a three-electrode cell configuration with a Ag/AgCl reference electrode (ET072, eDAQ) and Pt mesh counter electrode. The potential of the Ag/AgCl reference electrode was checked daily against a reversible hydrogen electrode (HydroFlex®, Gaskatel).

A custom-made, gas-tight two compartment polytetrafluoroethylene cell was used for CO_2 reduction experiments.[4] The anodic and cathodic compartments were separated by an anion-exchange membrane (Selemion AMV, AGC Asahi Glass). A holder gripped the working electrode firmly in place and exposed only a circular geometric surface area of 0.385 cm^2. The cathodic compartment was filled with 32 ml electrolyte, leaving approximately 3 ml of headspace. Before each measurement, the aqueous 0.1 M $KHCO_3$ (99.99%, Sigma Aldrich) electrolyte was saturated with CO_2 gas (99.999%, Linde Gas) for at least 30 minutes. All experiments were performed at 298 K.

CO_2 was continuously pumped into both the catholyte and anolyte during the CO_2 reduction process at a rate of 20 sccm using calibrated mass flow controllers (MC-100SCCM-D, Alicat Scientific). The gas outlet of the cathodic compartment was connected to a gas chromatograph (GC-7890A, Agilent Technologies) for periodical sampling. The GC is equipped with a thermal conductivity detector (TCD) for detecting H_2 and two flame ionization detectors (FID, one fitted with a methanizer) for detecting hydrocarbons and CO. The carrier gases for the TCD and FIDs are nitrogen and helium respectively. The GC was calibrated regularly using standard gas mixtures (Singapore Oxygen Air Liquide and National Oxygen Pte Ltd) at standard conditions (1 atm, 298 K).

A typical CO_2 electroreduction experiment at a constant applied voltage spanned over 4200 seconds. A total of six gas aliquots (2.5 cm^3 each) were measured. They were injected into the GC every 10 minutes by an automated sampler. The first

injection is 230 seconds after the start of the CO_2 reduction reaction; this ensures adequate flushing of the transfer line of atmospheric contaminants. The GC data collected in this work are translated to Faradaic efficiencies (FE) (supplementary information section S1). The Faradaic efficiencies of the products in all measurements amount to ~90% or better, which demonstrates that all the major electroreduction products have been detected.

NMR detection of formate

After each CO_2 electroreduction experiment, 2 mL of the catholyte was mixed with 0.1 mL of an internal standard consisting of 25 mM phenol (99.5%, Scharlau) and 5 mM dimethyl sulfoxide (99.9%, Quality Reagent Chemical). 0.5 mL of this aqueous mixture was then added to 0.7 mL D_2O (99.96% deuterium, Cambridge Isotope Laboratories). Solvent suppression was used to decrease the intensity of the water peak. Results presented here are average of 52 1D ^{1}H NMR scans (Avance 300, Bruker) and processed using WIN-NMR software (Bruker). Formate (chemical shift 8.3 ppm) was the only CO_2 reduction product detected in the electrolyte.[4]

Characterization of Copper Catalysts

The surface morphologies of the Cu catalysts were analyzed by scanning electron microscopy (SEM, JEOL JSM-6710F) operated in secondary electron mode (5 keV, 10 mA probe current). High resolution transmission electron micrographs of selected catalysts were obtained using JEOL TEM-3010. For the TEM measurements, the top layer of the Cu samples were scraped off the substrate and suspended in isopropanol using ultrasonication. A drop of the homogenized solution was then drop-casted on a 300 mesh nickel grid coated with lacy carbon (LC325-Ni, Electron Microscopy Sciences). Only smaller particles, with sizes ≤50 nm, could be analyzed by TEM as the electron beam cannot penetrate through larger particles.

X-ray photoelectron spectroscopy (XPS) was performed using a Kratos AXIS Ultra (Al Kα emission source). An ultrathin Pt film was sputter-coated onto the catalyst surface just before XPS measurement as internal standard for binding energy calibration. X-ray diffractions (XRD) of the films were performed on Bruker D8 (Cu Kα, 40 kV, 40 mA). The incoming X-ray angle was kept at 0.1° to minimize the diffraction signal from the underlying copper disc.

iR Drop Compensation and Reporting of Working Electrode Potentials and Currents

iR drop compensation was made during the electrochemical measurements using the current interrupt technique. All the potentials measured in this work are referenced to the RHE using the following conversion:

$$E_{RHE}\ (V) = E_{Ag/AgCl}\ (V) + 0.205\ V + (0.059\ V \times pH)$$

The pH values of the electrolytes are listed in supplementary information S2. The current density values reported in this work were normalized to the geometric surface area.

Results and Discussion

GC results: Stable Ethylene Selectivity on Copper Mesocrystals

Representative chronoamperograms of Catalysts A, B and C (A = Cu mesocrystals, B = Cu nanoparticles and C = electropolished Cu) during CO_2 electroreduction at -0.99 V are presented in Figure 1A. Catalyst A exhibited significantly higher reduction current during the first ~200 seconds that peaked at -65 mA cm^{-2} before stabilizing to *ca.* -25 mA cm^{-2}.

On the basis of ex-situ characterization of Catalyst A at

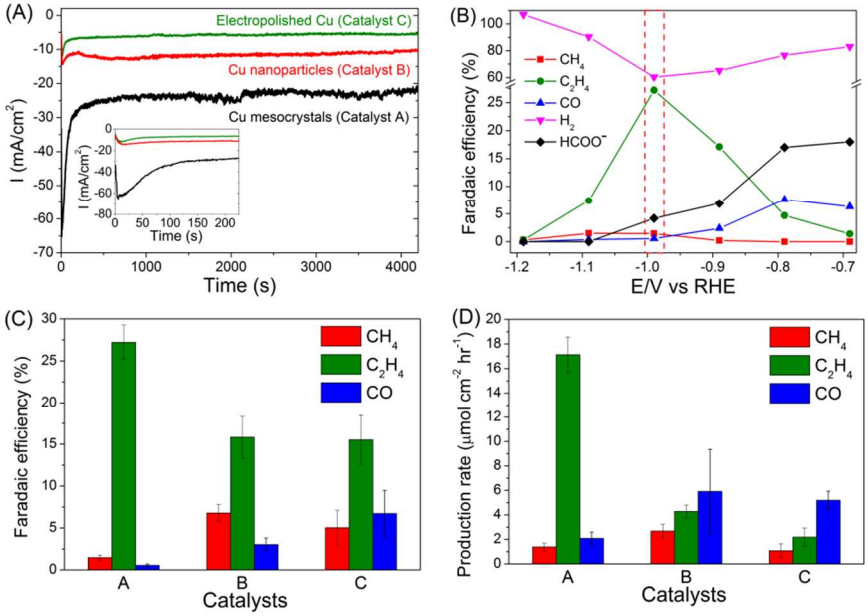

Fig. 1 (A) CO_2 reduction current as a function of time for Catalysts A (Cu mesocrystals), B (Cu nanoparticles) and C (electropolished Cu). Potential applied: -0.99 V. The insert is a zoomed-in picture of the reduction currents at the start of the CO_2 reduction process. (B) Faradaic efficiencies for the CO_2 electroreduction products of Catalyst A as a function of potential. A comparison of the (C) Faradaic efficiencies and (D) production rates of CO_2 electroreduction products on Catalysts A, B and C at -0.99 V.

different times during the electrochemical CO_2 reduction (see the following section), this temporal reduction current was attributed to the reduction of CuCl to Cu mesocrystals. When steady state currents were compared, Catalyst A always displayed the highest current density, which is approximately twice and three times that of Catalysts B and C respectively (supporting information section S3). We have determined, from their cyclic voltammograms, that the ratio of electroactive surface areas of Catalysts A, B and C is approximately 5:2:1. Hence, the difference in measured currents can be attributed to differences in surface areas of the catalysts.

The detected products in Catalysts A, B and C are methane, ethylene, carbon monoxide, formate and hydrogen, and their Faradaic efficiencies vary with the applied working potentials (Fig. 1B, supporting information section S4). Strikingly, only Catalyst A exhibited significant preference towards C_2H_4 formation. At -0.99 V, the FE of C_2H_4 and CH_4 are 27.2% and 1.47% respectively, which gives C_2H_4/CH_4 ratio of ~18 (Fig. 1 B-C). This ratio is greater than the C_2H_4/CH_4 selectivity of ~10 found for high-indexed $(711)_{Cu}$ single crystal copper surfaces.[7] As a comparison, Catalysts B and C exhibit C_2H_4/CH_4 ratios of only 2.3 and 3.1 respectively, consistent to the ratios reported previously on polycrystalline and sputtered Cu electrodes (Fig. 1C).[4-6, 20] C_2H_6 was also detected on Cu mesocrystals, with Faradaic efficiency of ~0.3 %, (supporting information section S1) but not on the other two catalysts. The Faradaic efficiency of C_2H_4 formation from Catalyst A is ~81% of the total carbonaceous products yield (Fig. 1C). This is significantly higher than the C_2H_4 yield of 45% and 40% found on Catalysts B and C. This figure is also higher than the 61% C_2H_4 yield found on $(711)_{Cu}$.[7] In terms of production rate, C_2H_4 is produced at a rate of ~17 μmol cm^{-2} hr^{-1} using Catalyst A (Fig. 1D). This is approximately an order of magnitude higher than that observed for Catalyst C. These figures of merit demonstrate that there is a significant improvement to the selectivity of CO_2 reduction to C_2H_4 when Cu mesocrystal catalysts are used.

The rapid deactivation of the Cu catalysts is a major obstacle that will hinder any efforts to industrially scale up the CO_2 electroreduction process to produce C_2H_4.[8, 9] It is therefore important to assess the stability of our copper electrodes over longer CO_2 electroreduction periods. A bias of -0.99 V was chosen as it showed optimum selectivity towards C_2H_4, especially for copper mesocrystals (Catalyst A, Fig. 1B). Results presented in Fig. 2 demonstrate that the copper mesocrystals displayed both superior and stable catalytic activity towards C_2H_4 formation for >6 hours (Fig. 2A). In contrast, Catalysts B and C showed rapid catalytic deactivation. The Faradaic efficiencies of their CH_4 and C_2H_4 products declined over the course of the electrolysis, with the FE of C_2H_4 of Catalyst C decreasing by 75%. H_2 production has also increased for these two catalysts. Deactivation of Cu catalysts has been previously attributed to contamination from trace amounts of heavy metals present in the electrolyte.[8] Subsequent sections of this work will be devoted to in-depth materials and electrochemical investigation of the origin of the higher ethylene selectivity and stability of our Cu mesocrystals catalyst.

Chemical and Structural Analysis of the Cu Mesocrystals

Cu mesocrystals (Catalyst A) were analyzed before, during and after CO_2 reduction. The initial steps of Cu mesocrystals formation involve five cycles of electrochemical roughening of the polished Cu disc in 0.1 M KCl solution. After this roughening procedure, aggregated particles of ~400-1000 nm in size were found on top of the polished Cu (Fig. 3A-B). X-ray diffraction and XPS revealed that these particles are CuCl (Fig. 3C-D). The CuCl-covered Cu disc was then rinsed in deionized water and used directly for electrochemical CO_2 reduction.

Within 10-20 seconds from the application of -0.99 V to the electrode in CO_2-saturated $KHCO_3$, the CuCl layer were converted to cuboids of approx. 400-500 nm across (Fig. 3E). A longer exposure time (~100 seconds) resulted in the growth of smaller 30-50 nm nanoparticles over the well-defined cuboids' surface (Fig. 3F-H; see also supplementary information section S5).

These small and rough nanoparticles were determined by XRD and XPS to be crystalline copper metal (Fig. 3C-D). No CuCl, Cl, or metal contaminants such as Fe or Zn could be detected on the catalyst's XPS spectra after 4200 seconds of CO_2 electrochemical reduction process. As there should be no Cu ions present in the $KHCO_3$ electrolyte initially, the formation of Cu mesocrystals from CuCl must have proceeded via a dissolution-redeposition[21] followed by oriented attachment[22] or a self-limiting electrochemical aggregative growth mechanism,[23] with the large Cu cuboids surface acting as an orientation template.[24]

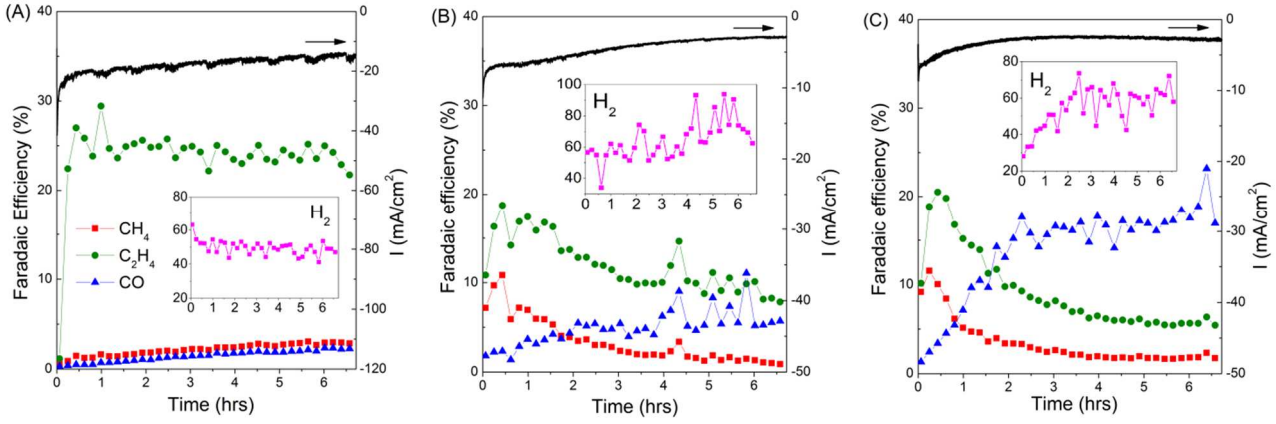

Fig.2: Composite plot of current density vs. time (black trace) at -0.99 V and Faradaic efficiencies of CO (blue trace), C_2H_4 (green), CH_4 (red) and H_2 (inset, magenta), over six hours of CO_2 reduction for: (A) Catalyst A, (B) Catalyst B, and (C) Catalyst C.

Representative high resolution transmission electron micrograph of the 30-50 nm Cu nanoparticle clusters, obtained by scraping Catalyst A after 4200 seconds of CO_2 electroreduction is shown in the Fig 3I. The marked *d*-spacings in these nanoparticles correspond to those of Cu metal only (Fig. 3J).‡ The most striking observation in the HRTEM images is the clear presence of numerous atomic steps and $(100)_{Cu}$ terraces on the surfaces of these copper nanoparticles (Fig. 3K-L, also see supplementary information S6). This arrangement is reminiscent of the high-indexed facet exposed by off-cutting $(100)_{Cu}$ single crystals, exposing numerous high-indexed atomic steps with $(100)_{Cu}$ terraces in between.[7] However, as our Cu mesocrystals have larger surface areas than single crystal copper surfaces, there will be significantly more high-indexed atomic steps. The $(100)_{Cu}$ surface terminations of the Cu mesocrystals may have been promoted by the underlying Cu cuboid template when it was formed from CuCl (Fig. 3E). Such process usually has a lower activation energy.[25] Similar mesocrystals were also observed after CO_2 electroreduction at different potentials between -0.69 and -0.89 V (supplementary information section S7). We thus conclude that the selective reductions of CO_2 to ethylene at other potentials, while showing variable product ratios, were catalyzed by the same Cu mesocrystals.

Catalyst B (Cu nanoparticles) was introduced to assess the importance of the well defined cuboid surface (in Fig. 3E) as templates for the mesocrystals to nucleate and arranged as mesocrystals. These electrodeposited copper nanoparticles are relatively small, and possess high surface areas (Fig. 4A-B). However, as they were grown directly on polycrystalline copper discs, which do not have significant number of exposed $(100)_{Cu}$ growth template like Catalyst A, this results in rounded particles without any clear $(100)_{Cu}$ termination. This morphology was retained throughout the CO_2 reduction at -0.99 V (Fig. 4C). High resolution TEM revealed that the surfaces of these rounded nanoparticles were smoothly gradated, possibly with many steps, but no terraces could be found (Fig. 4D inset, see also supplementary information S8). This surface can thus be classified as an extremely high indexed plane with many steps but with no terraces. While Hori et al. have shown that high-indexed stepped surfaces are important for C_2H_4 selectivity, exposing even higher indexed plane than $(711)_{Cu}$ appears to be detrimental to C_2H_4 selectivity.[7] This suggests that $(100)_{Cu}$ terraces are important and high C_2H_4 selectivity can only be achieved by balancing the steps and terrace population. Thus unsurprisingly, Catalyst B only displayed C_2H_4/CH_4 ratio of 2.3, not very different from a regular polycrystalline copper.[4]

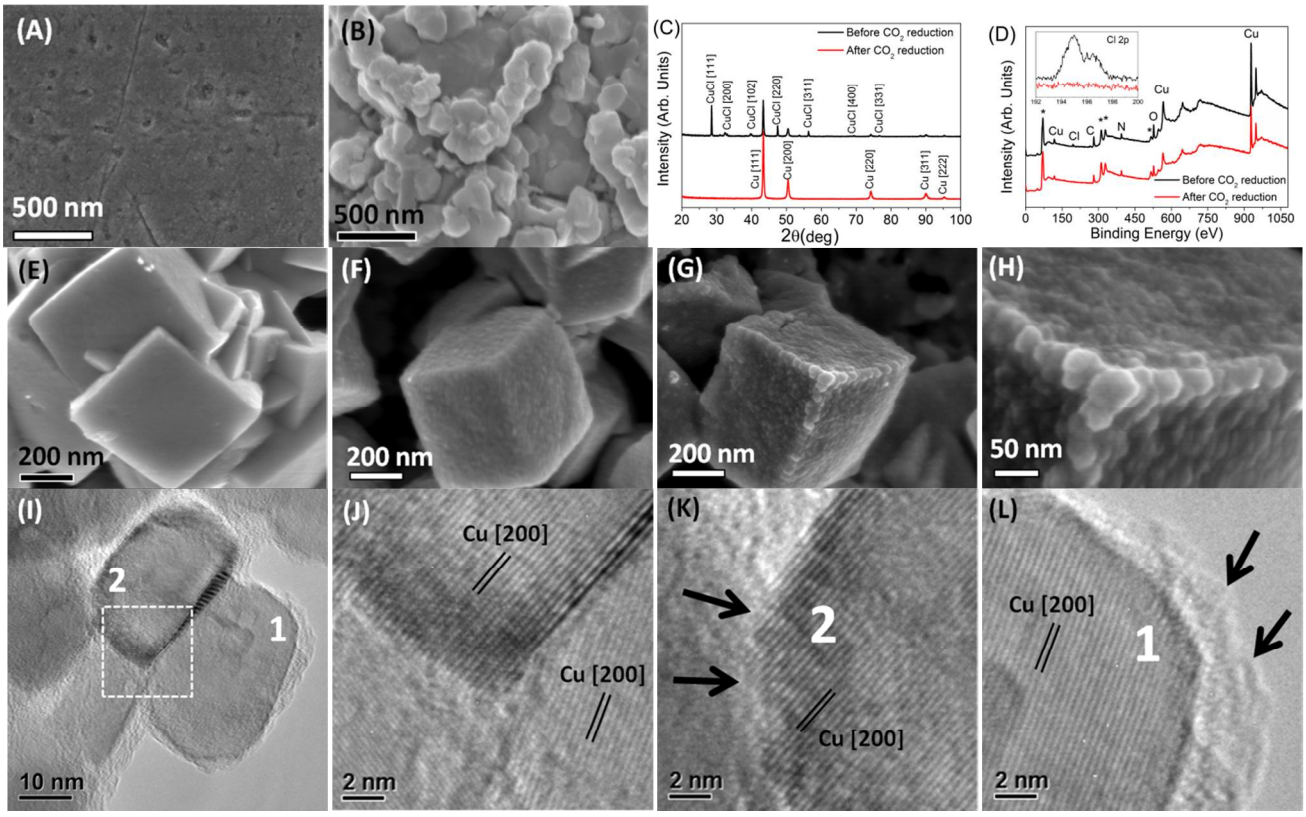

Fig. 3: SEM micrographs of (A) polished Cu and (B) Catalyst A before CO_2 reduction. (C) X-ray diffraction and (D) XPS data of Catalyst A before (black trace) and after 4200 seconds of CO_2 reduction (red trace). The asterisks indicate internal Pt standard. The insert in panel (D) shows a zoomed-in region where the Cl 2p XPS peak occurs. Time resolved ex-situ SEM micrographs of Catalyst A after: (E) 10, (F) 100, and (G-H) 4200 seconds of CO_2 electroreduction. (I-L) HRTEM micrographs of the same catalysts in (G-H) with increasing magnifications. Only lattice parameters belonging to Cu metal were detected. Dark arrows indicate some of the steps and edges present on the Cu mesocrystals.

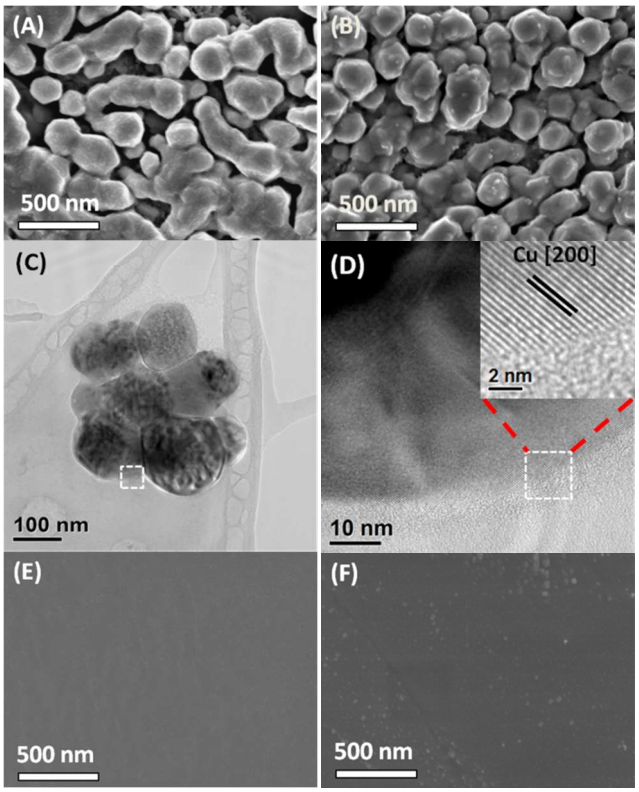

Fig. 4: SEM micrographs of electrodeposited copper nanoparticles (A) before and (B) after CO_2 reduction. (C) A representative HRTEM micrograph of electrodeposited Cu nanoparticles after CO_2 reduction. (D) Increased magnification of marked area in (C). SEM micrographs of the electropolished Cu surface (E) before and (F) after CO_2 reduction.

Catalyst C was introduced to represent smooth polycrystalline Cu surfaces. As seen in Fig 4E, electropolishing strips the Cu surface of protrusions by dissolving them into phosphoric acid, resulting in a very smooth surface. As a result, Catalyst C was not found to be selective towards C_2H_4 formation, which is in agreement with previous reports on polycrystalline copper.[4, 5]

After CO_2 reduction, the surface becomes slightly rougher with newly formed protrusions (Fig. 4F). The roughening could be attributed to the prolonged application of cathodic potentials. However, this roughened surface does not exhibit any selectivity towards C_2H_4 (Fig. 2C).

CO Adsorption Studies and Robustness of Cu Mesocrystals

Thus far, we have demonstrated that copper mesocrystals are highly selective towards the electrocatalytic reduction of CO_2 to C_2H_4. We have also established, by comparing different copper surfaces, that the presence of both $(100)_{Cu}$ facets and atomic steps / edges are essential for this selectivity.

The dimerization of CO (or CHO*) on copper has been postulated to be the key step for C_2H_4 formation during CO_2 reduction.[26-28] This suggests that the population of active sites responsible for C_2H_4 formation can be probed by CO adsorption.

Baseline measurements of these three catalysts in Ar-saturated 0.1 M $KHCO_3$ were first taken. The oxidation and reduction potentials of the Cu catalysts in all three catalysts agree well with previous reports (Fig. 5A).[6] Cu mesocrystals (Catalyst A) show

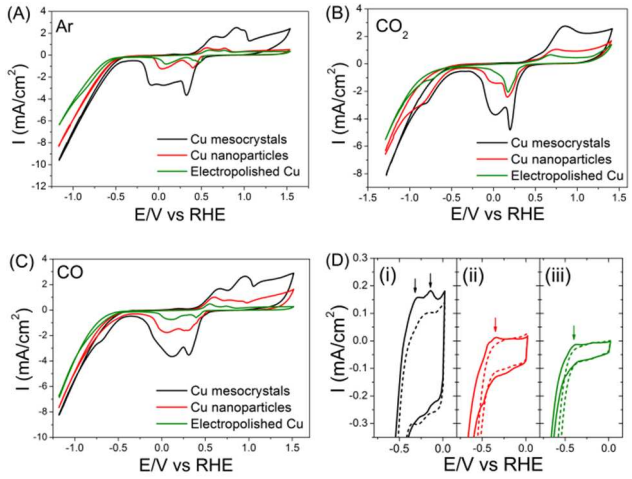

Fig. 5: Cyclic voltammograms of the three Cu catalysts in (A) Ar-, (B) CO_2- and (C) CO-saturated 0.1 M $KHCO_3$. (D) Close comparison of the CVs of (i) Cu mesocrystals, (ii) Cu nanoparticles and (iii) electropolished Cu in Ar- (broken line) and CO- (solid line) saturated 0.1 M $KHCO_3$. Arrows indicate CO adsorption/desorption features around -0.14 V (only on Cu mesocrystals) and -0.35 V (on all samples). These CV measurements were done after 4200 seconds of CO_2 electroreduction.

the highest current density and a more complex set of oxidation/reduction peaks. These observations can be respectively attributed to its larger surface area and to the greater number of exposed steps/facets on its surface.[6, 29] The CV measurements in CO- and CO_2- saturated electrolytes were very similar (Fig. 5B-C), which suggests that these two compounds can react similarly on Cu surfaces.[20] The shoulders at -0.7 to -0.9 V in the CVs shown in Fig. 5B-C are usually attributed to the formation of adsorbed CO.[30] However, more recent work by Kortlever *et al.* indicates that this peak is instead related to the direct reduction of bicarbonate to formate.[31]

When the CVs of the electrodes in CO-saturated electrolyte were examined between 0 to -0.5 V, an anodic peak feature around -0.14 V was observed exclusively on the Cu mesocrystals (Fig. 5D(i)). In contrast, both the Cu nanoparticles and electropolished Cu showed only a faint peak at -0.35 V. These peaks are reminiscent to the CO adsorption/desorption features observed in single crystal copper surfaces.[7] The more positive position and greater peak intensity in the CV of the Cu mesocrystals indicates that it adsorbs CO more readily as compared to the other two catalysts.[32]

Since dimerization of CO (or CHO*) is a key step in ethylene production, the fact that CO can be better adsorbed on the Cu mesocrystals can explain its preferred selectivity for ethylene production. The likely consequence is that CO and CH_4 products would be correspondingly lower on the Cu mesocrystals. This was indeed what we observed (Fig. 1D). The Faradaic efficiency of CO during CO_2 electroreduction on different Cu single crystal surfaces has also been shown to be inversely proportional to that of C_2H_4 in the literature.[7]

Unlike Catalysts B and C, Catalyst A's C_2H_4 production rate is constant throughout six hours (Fig. 2). A reason for this enhanced stability could be the minimum exposure of the Cu mesocrystals to the atmosphere as they were formed *in-situ* from CuCl during the CO_2 reduction process. However, we found that Catalyst A remained very active even when it was taken out mid reaction,

exposed to ambient atmosphere for several minutes, and then reintroduced back to the cell for further CO_2 reduction (supporting information section S9). Presence of Cl^- has also been reported to alter product selectivity in CO_2 electroreduction.[3, 16] However, we found that the activity and product distribution of CO_2 reduction on the Cu mesocrystals was not affected by Cl^- added to the $KHCO_3$ electrolyte (supporting information S9). These experiments demonstrate that the Cu mesocrystals are inherently more stable and resistant to atmospheric and trace contaminants than ordinary Cu surfaces or nanoparticles.

Conclusion

In this work, we report the highly selective and stable electroreduction of CO_2 to C_2H_4 on Cu mesocrystals. A C_2H_4/CH_4 FE ratio of ~18 was achieved. The *in-situ* formation of this novel electrocatalyst from CuCl resulted in mesostructurally arranged 30-50 nm $(100)_{Cu}$ terminated particles bearing many steps and edges. These specific surface arrangements lead to higher availability of active sites on Cu mesocrystals, indicated by higher and stronger CO- adsorption, a crucial factor that led to high C_2H_4 selectivity

Control CO_2 electroreduction experiments on electrodeposited Cu nanoparticles and electropolished Cu could not replicate the high C_2H_4 selectivity exhibited by Cu mesocrystals. Despite having large surface areas, electrodeposited Cu nanoparticles appeared more rounded and did not exhibit clear $(100)_{Cu}$ facets or terraces. These displayed similar product distribution as electropolished Cu surface. These control experiments affirmed that the presence of $(100)_{Cu}$ with steps as imaged in the Cu mesocrystals are indeed *essential* for the selective reduction of CO_2 to C_2H_4.

Most remarkably, our Cu mesocrystals are stable and selective towards C_2H_4 for over *six hours*. Exposure to chloride anions during reaction or atmospheric contaminants also does not significantly change the catalytic activity of the Cu mesocrystals. We believe that the development of facilely prepared, stable and selective Cu mesocrystals is a significant step towards the realization of industrial-scale CO_2 reduction to ethylene.

Acknowledgement

This work is supported by a start-up grant (R143-000-515-133) from the National University of Singapore. A.D.H. is grateful for a research fellowship from Singapore-Peking-Oxford Research Enterprise (R-706-000-100-414)

The authors thank Dr. Yuan Ze Liang (NUS Chemical and Biomolecular Engineering) for XPS measurements and Mr. Lee Ka Yau (NUS Chemistry) for TEM measurements.

Notes and references

[a] *Department of Chemistry, National University of Singapore, 3 Science Drive 3, Singapore 117543. Fax: (65)-67791691; Tel: (65)-65162836; E-mail: chmyeos@nus.edu.sg*

† Electronic Supplementary Information (ESI) available: Calculation of Faradaic efficiencies, representative raw data, electron micrographs and electrochemical data. See DOI: 10.1039/b000000x/

‡ $(200)_{Cu}$ is an equivalent plane to $(100)_{Cu}$ but with half the lattice spacing. Note that Cu has a $Fm\bar{3}m$ spacegroup which only allows $(l00)$ reflexions to be seen in X-ray or TEM diffraction when l is even (l=2n). Thus we observe $(200)_{Cu}$ and not $(100)_{Cu}$ in Fig. 3C (XRD) and Fig. 3J-L (HRTEM). The same explanation is also applicable for $(220)_{Cu}$ and $(110)_{Cu}$.

1. D. T. Whipple and P. J. A. Kenis, *J. Phys. Chem. Lett.*, 2010, **1**, 3451-3458.
2. Y. Hori, H. Wakebe, T. Tsukamoto and O. Koga, *Electrochim. Acta*, 1994, **39**, 1833-1839.
3. Y. Hori, in *Modern Aspects of Electrochemistry*, eds. C. Vayenas, R. White and M. Gamboa-Aldeco, Springer New York, 2008, vol. 42, ch. 3, pp. 89-189.
4. K. P. Kuhl, E. R. Cave, D. N. Abram and T. F. Jaramillo, *Energy Environ. Sci.*, 2012, **5**, 7050-7059.
5. Y. Hori, A. Murata and R. Takahashi, *J. Chem. Soc., Faraday Trans. 1*, 1989, **85**, 2309-2326.
6. W. Tang, A. A. Peterson, A. S. Varela, Z. P. Jovanov, L. Bech, W. J. Durand, S. Dahl, J. K. Norskov and I. Chorkendorff, *Phys. Chem. Chem. Phys.*, 2012, **14**, 76-81.
7. Y. Hori, I. Takahashi, O. Koga and N. Hoshi, *J. Mol. Catal. A: Chem.*, 2003, **199**, 39-47.
8. Y. Hori, H. Konishi, T. Futamura, A. Murata, O. Koga, H. Sakurai and K. Oguma, *Electrochim. Acta*, 2005, **50**, 5354-5369.
9. D. W. DeWulf, T. Jin and A. J. Bard, *J. Electrochem. Soc.*, 1989, **136**, 1686-1691.
10. K. J. P. Schouten, E. Pérez Gallent and M. T. M. Koper, *J. Electroanal. Chem.*, 2014, **716**, 53-57.
11. K. J. P. Schouten, E. Pérez Gallent and M. T. M. Koper, *ACS Catal.*, 2013, **3**, 1292-1295.
12. C. W. Li and M. W. Kanan, *J. Am. Chem. Soc.*, 2012, **134**, 7231-7234.
13. M. Gattrell, N. Gupta and A. Co, *J. Electroanal. Chem.*, 2006, **594**, 1-19.
14. Y. Hori, I. Takahashi, O. Koga and N. Hoshi, *J. Phys. Chem. B*, 2001, **106**, 15-17.
15. J. Yano, T. Morita, K. Shimano, Y. Nagami and S. Yamasaki, *J. Solid State Electrochem.*, 2007, **11**, 554-557.
16. K. Ogura, H. Yano and F. Shirai *J. Electrochem. Soc.*, 2003, **150**, D163-D168.
17. W. J. Durand, A. A. Peterson, F. Studt, F. Abild-Pedersen and J. K. Nørskov, *Surf. Sci.*, 2011, **605**, 1354-1359.
18. R. Kas, R. Kortlever, A. Milbrat, M. T. M. Koper, G. Mul and J. Baltrusaitis, *Phys. Chem. Chem. Phys.*, 2014, **16**, 12194-12201.
19. B. S. Yeo and A. T. Bell, *J. Am. Chem. Soc.*, 2011, **133**, 5587-5593.
20. Y. Hori, H. Wakebe, T. Tsukamoto and O. Koga, *Surf. Sci.*, 1995, **335**, 258-263.
21. L. Yu, H. Sun, J. He, D. Wang, X. Jin, X. Hu and G. Z. Chen, *Electrochem. Commun.*, 2007, **9**, 1374-1381.
22. E. J. H. Lee, C. Ribeiro, E. Longo and E. R. Leite, *J. Phys. Chem. B*, 2005, **109**, 20842-20846.
23. J. Ustarroz, J. A. Hammons, T. Altantzis, A. Hubin, S. Bals and H. Terryn, *J. Am. Chem. Soc.*, 2013, **135**, 11550-11561.
24. M. Tian, J. Wang, J. Kurtz, T. E. Mallouk and M. H. W. Chan, *Nano Lett.*, 2003, **3**, 919-923.
25. K. R. Sarma, P. J. Shlichta, W. R. Wilcox and R. A. Lefever, *J. Cryst. Growth*, 1997, **174**, 487-494.

26. K. J. P. Schouten, Y. Kwon, C. J. M. van der Ham, Z. Qin and M. T. M. Koper, *Chem. Sci.*, 2011, **2**, 1902-1909.
27. F. Calle-Vallejo and M. T. M. Koper, *Angew. Chem. Int. Ed.*, 2013, **52**, 7282-7285.
28. A. A. Peterson, F. Abild-Pedersen, F. Studt, J. Rossmeisl and J. K. Norskov, *Energy Environ. Sci.*, 2010, **3**, 1311-1315.
29. A. Hamelin and A. M. Martins, *J. Electroanal. Chem.*, 1996, **407**, 13-21.
30. Y. Hori, A. Murata, R. Takahashi and S. Suzuki, *J. Chem. Soc., Chem. Commun.*, 1988, 17-19.
31. R. Kortlever, K. H. Tan, Y. Kwon and M. T. M. Koper, *J. Solid State Electrochem.*, 2013, **17**, 1843-1849.
32. S. K. Shaw, A. Berna, J. M. Feliu, R. J. Nichols, T. Jacob and D. J. Schiffrin, *Phys. Chem. Chem. Phys.*, 2011, **13**, 5242-5251.